Water Reuse

Enhanced desalination efficiency of flow-through capacitive deionization cell by mesh electrode with granular aerogel carbon in the removal of ions from synthetic and real samples

Bahram Roshan[a], Hassan Rasoulzadeh [a,b,*], Mohamadreza Massoudinejad[a], Mohsen Saadani[a] and Daryoush Sanaei[a]

[a] Department of Environmental Health Engineering, School of Public Health and Safety, Shahid Beheshti University of Medical Sciences, Tehran, Islamic Republic of Iran
[b] Student Research Committee, Department of Environmental Health Engineering, School of Public Health and Safety, Shahid Beheshti University of Medical Sciences, Tehran, Islamic Republic of Iran
*Corresponding author. E-mail: hasanrseng@gmail.com

HR, 0000-0002-9539-6946

ABSTRACT

Flow-through capacitive deionization (FTCDI) is a traditional improved flow-by CDI cellular structure, used to remove ions from aqueous solutions. In this study, a new FTCDI was designed consisting of mesh electrodes (ME) containing ion-exchange membranes (IEM) and aerogel carbon granules with a specific surface area of 489 m^2/g. All analyses and experiments performed showed that the new design can remove nitrate, phosphate, sodium, calcium, and chloride. Under optimal conditions, the new FTCDI system can remove 82.5, 49, 85, and 90% of sodium chloride, calcium chloride, nitrate, and phosphate with a maximum input concentration of 450 mg/L, 450 mg/L, 70 mg/L, and 3 mg/L, respectively. The efficiency of this system was also evaluated for real samples. Findings of the study showed that if the initial amount of turbidity is 12 NTU, total soluble solids (TDS) 1,700 mg/L, total hardness 540 mg/L, phosphate 0.09 mg/L, nitrate 28.8 mg/L, and electrical conductivity (EC) 3,480 μs/cm, the system can remove 25, 23.5, 33.3, 66.6, 54.4, and 39.1%, respectively.

Key words: capacitive deionization cell, desalination, granular aerogel carbon

HIGHLIGHTS

- Novel FTCDI system was designed.
- The designed FTCDI was utilized for nitrate, phosphate, sodium and calcium chloride removal from synthetic solutions.
- It was also utilized for nitrate, phosphate, sodium and calcium chloride removal from real samples.
- FTCDI influential parameters were investigated.
- Studied system exhibited excellent deionization performance.

1. INTRODUCTION

Only 3% of the total surface water resources are in the form of surface water. The results of various studies show more than three billion people in 150 countries use desalination processes due to insufficient access to drinking water resources (Panagopoulos & Haralambous 2020). In this case, desalination seems to be a promising alternative. Desalination is the application of several different steps in saline water to remove or reduce excess salts and minerals (Panagopoulos 2021). Now, common technologies, such as reverse osmosis (RO), nanofiltration (NO), and thermal distillation (multi-stage flash (MSF) and multi-effect distillation (MED) are used despite high-energy consumption and environmental problems to purify and desalinate saline water sources (Panagopoulos 2020).

Although, owing to their energy consumption, brine discharge, and greenhouse gases emissions, these methods are not proper alternatives for the desalination from saline solutions (Xing et al. 2020; Ihsanullah et al. 2021). In the past decades, electrochemical technologies have been introduced as a more reliable alternative to desalination of brackish water sources due to less energy consumption compared to conventional methods (Tang et al. 2020). Capacitive deionization (CDI) is

one of these emerging technologies (Xing *et al.* 2020). This process has various advantages compared to conventional processes, such as greater safety, no need for high-pressure pump, working at low voltage (1.8 < V), no need for a chemical to regenerate, short system wash time, energy saving, cost-effective, and very environmentally friendly (Choi *et al.* 2019). The most important advantage of the system compared to other systems is its energy consumption efficiency which is, on average, 0.1 to 1.5 kWh/m^3 of deionized water. Such advantages have led to the proposed method, among conventional methods, as a reliable alternative to the removal of soluble substances from brackish water (Pan *et al.* 2020).

The most common CDI cellular structure, which is known as flow-by CDI or flow-between CDI electrodes (Baroud & Giannelis 2018), consists of a pair of electrodes (anode and cathode electrodes). To prevent short-circuiting, this pair of electrodes includes an adsorbent and a non-conducting layer installed between two electrodes with opposite charge (Tang *et al.* 2016; Kalfa *et al.* 2020). The general principles of the CDI system consist of two stages of adsorption and desorption (AlMarzooqi *et al.* 2014). The solution containing ions is passed between the two carbon electrodes, and the positively charged ions are absorbed by the cathode electrode and the negatively charged ions are adsorbed by the anode electrode, Finally, ion-free water (pure) is passing out between the two electrodes (Biesheuvel & Van der Wal 2010; Chen *et al.* 2020). Once these electrodes are saturated, they can be regenerated by zeroing the voltage or reversing the voltage current, and releasing adsorbed ions into the brine (Wang & Lin 2019). Previous studies have focused on the development of electrode materials, increasing the adsorption capacity of electrodes, improving energy efficiency, and determining optimal CDI conditions (Kim *et al.* 2019; Wang *et al.* 2019; Zhao *et al.* 2020). The results of these studies led to the formation of various CDI cell structures (Tang *et al.* 2019). One of these structures is the flow-through electrode capacitive deionization (FTCDI) cell, where the solution passes directly through the macropores of the electrode, unlike other structures (Andelman 2011; Guyes *et al.* 2017), allowing more contact between the dissolved ions, the adsorbent and the electrodes (Tang *et al.* 2017; Son *et al.* 2020). This procedure increases the efficiency of the electrodes in the adsorption phase compared to CDI and MCDI (Remillard *et al.* 2018). On the other hand, this system, unlike CDI and MCDI, cannot use the voltage reversal method in the regeneration phase because of the simultaneous occurrence of the adsorption process (re-absorption of co-ions by the opposite electrode) and desorption. It can only use the zero voltage method, but this method reduces the capacity of the electrodes over time (Zhang *et al.* 2019a, 2019b; Algurainy & Call 2020). Moreover, the previous researches have focused on the removal of an ion from solutions. This created a study gap in using CDI systems for real samples (Algurainy & Call 2020; Pan *et al.* 2020). Therefore, a basic study is needed to investigate the removal of all ions from different aqueous solutions such as saline water, municipal wastewater, industrial wastewater, etc.

Based on the above, the overall purpose of this study was to investigate the simultaneous removal of several different ions in synthetic and real samples. In this study, a new FTCDI cell structure has been designed to enhance its performance. Moreover, the designed system can use the voltage reversal method to regenerate the electrodes. To achieve this goal, an ion-exchange membrane (IEM) was used under each electrode and a protective plate in each cell. Therefore, an enhanced batch-FTCDI system with a new design of carbon aerogel electrodes was used to study its ability in the removal of sodium and calcium chloride, nitrate and phosphate ions in synthetic samples at specified concentrations and tap water.

2. MATERIALS AND METHODS

2.1. Synthesis of carbon aerogels

The principles of synthesis of aerogel carbon were similar to previous methods, except for the drying method, which includes three methods: supercritical drying, freeze-drying, or evaporation under vacuum (Zhang *et al.* 2019a, 2019b). Among the methods mentioned, the evaporation under vacuum drying method was selected due to the simplicity of work, low cost and risks and, on the other hand, considering the equipment available in the laboratory (Job *et al.* 2005). In the vacuum drying method, the materials required for the synthesis of aerogel carbon were first prepared according to the following molar ratios:

$$\frac{\text{Resorcinol}}{\text{Formaldehyde}} = 0.5 \rightarrow \frac{50\text{g}}{34\text{mL}}.$$

$$\frac{\text{Resorcinol}}{\text{Sodium Carbonate}} = 1000 \rightarrow \frac{50\text{g}}{0.048\text{lg}}.$$

$$\frac{\text{Distilled water}}{\text{Resorcinol} + \text{Formaldehyde} + \text{Sodium Carbonate}} = 5.7 \rightarrow 140\text{mL}$$

After preparing 50 g of primary material, depending on the amount of carbon required, resorcinol (R) (purity >99%) was gradually added to 100 mL of distilled water on a stirrer at 600 rpm. After complete dissolution of the resorcinol was achieved, 34 mL of formaldehyde (F) (37% wet, with 10% methanol) was added to it under the hood. In a separate container while the resorcinol solution was homogenizing, 0.0481 g of sodium carbonate was added to 40 mL of distilled water. The solution was slowly added to the solution of resorcinol and formaldehyde to form a bond between the molecules (Abolhasani et al. 2019). Finally, after 2 h at 600 rpm the solution becomes homogeneous. Next, the solution was poured into suitable cells. The cells were then placed in an oven at 85 °C for 72 h. The gel was removed from the oven and cooled to room temperature. The cooled gel was immersed in an acetone bath at 30.5 °C for 72 h. This is to allow the acetone to penetrate rapidly into the gel pores and exchange with the remaining water inside the tissue and gel pores. The acetone-containing gel was placed in a vacuum furnace (OV-12, Jiao tech, Seoul, Korea) at 105 °C at a pressure of −0.04 MPa for 48 h to remove the acetone from the aerogel tissue. To activate the aerogel, it was placed in a tube furnace (ATE1700 L Series Laboratory Tube Furnace, Iran) under contact with a continuous stream of nitrogen (140 mL/min) at 950 °C for 1 h to prevent the aerogel from turning gray. After the sample had cooled completely, it was again placed in a tubular furnace under contact with carbon dioxide gas for 1 h to reach a temperature of 950 °C. Finally, low-density black porous carbon was formed (Hwang & Hyun 2004). Carbon aerogel prepared by this method was divided into three diameter ranges of 0.9–1, 1–2, and 2–3 mm. Figure 1 schematically illustrates the synthetic route of aerogel carbon.
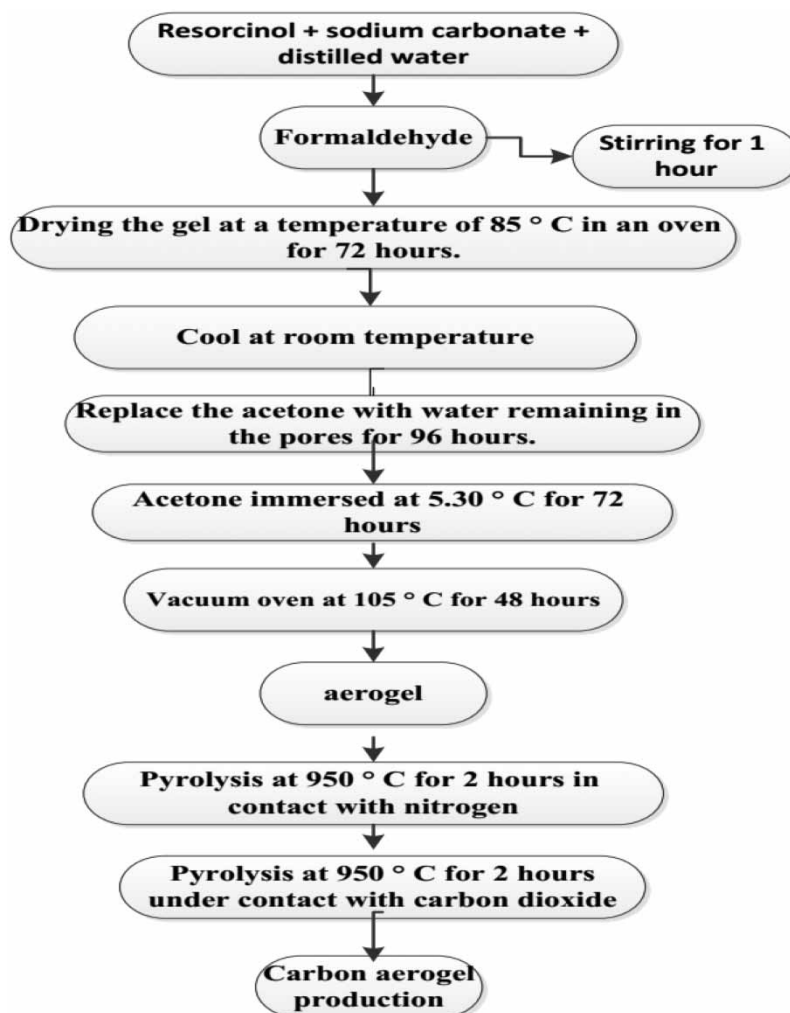

Figure 1 | Carbon aerogel synthesis steps.

2.2. Manufacture of electrodes and FTCDI system

Each mesh electrode consists of two circular mesh plates with an inner diameter of 5 cm and an outer diameter of 5.5 cm made of stainless steel with pores with a diameter of 0.9 mm, and containing 1 g of aerogel carbon granule between the two mesh plates. Under each electrode was an IEM with a diameter of 5.5 cm (manufactured by Fujifilm, the Netherlands) (Figure 2(b)). After the electrode was made, the FTCDI cell was prepared. Each cell consists of two electrodes prepared in the previous steps and a non-conductive ring made of Plexiglas, which was located to prevent short circuit current (Figure 2(c)). The next step is to build an FTCDI pilot with a diameter of 5.5 cm and a height of 15 cm in a cylindrical shape. This system consists of three FTCDI cells (six electrodes), with a total surface area of 2.934 m^2 and aperture volume of 1.824 cm (Figure 2(d)). Other components of the experimental FTCDI pilot (Figure 3) include a desalination solution and concentrate storage tank and a voltage source. An electric conductivity meter measures the concentration of ions. A peristaltic pump, with a capacity of 5 L/h, was used to regulate and circulate water flow regulate.

2.3. System operation FTCDI

As shown in Figure 3, an IEM was placed under each electrode. In other words, it was placed under the negative electrode of the anion exchange membrane (AEM) and below the positive electrode of the cation exchange membrane (CEM). These membranes cause more ions with opposite charges to be trapped in each electrode during the adsorption phase (increasing the adsorption efficiency compared to conventional FTCDI). The membranes allow only the ions with the same charge as electrode to pass through. For this reason, the adsorption efficiency in the FTCDI used is extended to the conventional FTCDI.

The reduction phase, in the FTCDI used, was done by reverse voltage method, in which the voltage reverses. In this system, the adsorption flow valves close and the washing flow opens at the same time. The co-ions of each electrode are released into the upper space and the presence of the shield plate prevents their re-adsorption with opposite charge electrodes, at which time the trapped co-ions are transferred to the brine tank by washing flow (Bian *et al.* 2015).

To determine the optimal condition of the FTCDI system (Figure 3) in batch conditions, sodium chloride concentration of 300 µs/cm (total sample volume 150 mL) was circulated between the FTCDI systems. A peristaltic pump (made in the USA) was circulating NaCl solution with the volume of 150 mL between the storage tank and system at different flow rates (80, 60, and 40 mL/min). Different voltages of 0, 0.8, 1, and 1.2 V were supplied by a voltage source, and to prevent Faradaic reactions, used voltage of less than 1.23 V. The effect of aerogel carbon granules with different diameters of 0.9–1, 1–2, and 2–3 mm was investigated. The electrical conductivity of sodium chloride solution was monitored every 2.5 min by an online conductivity meter. After the adsorption process, which usually takes between 30 and 40 min and circulates approximately four times per desalination test, the electrodes were regenerated with distilled water (100 mL) and the voltage reversed (5–10 min) until the electrodes reached their initial capacity. After determining the optimal conditions, the efficiency of the system in the removal of sodium (150, 300, and 450 mg/L) and calcium chloride ions (450 mg /L), nitrate (30, 50, and 70 mg/L), and phosphate (1, 2, and 3 mg/L) at different concentrations were studied. In the next step, to determine the efficiency of the process in removing these pollutants in real conditions, the experiments were evaluated using the city's drinking water samples. Deionization performance after each sampling (2.5 min) was evaluated by desalination efficiency (Equation
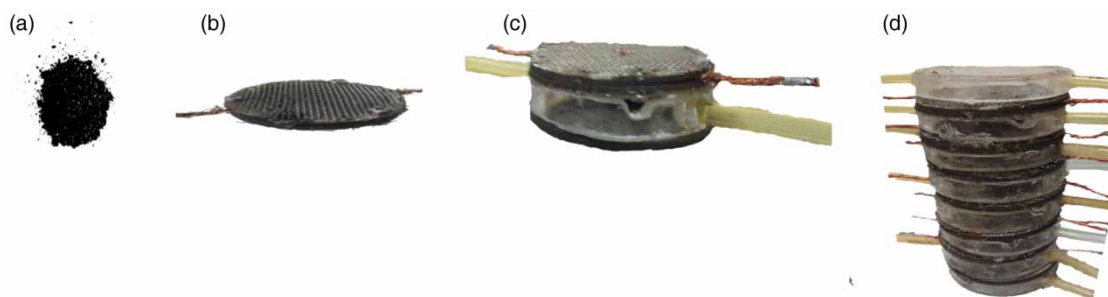

Figure 2 | (a) Aerogel carbon granules; (b) mesh electrode stainless steel two circular mesh plates with inner diameter of 5 cm, outer diameter of 5.5 cm with pores with a diameter of 0.9 mm and containing 1 g of carbon aerogel; (c) a cell consisting of two electrodes, a Plexiglas, and two ion exchange membranes; (d) three interconnected cells.
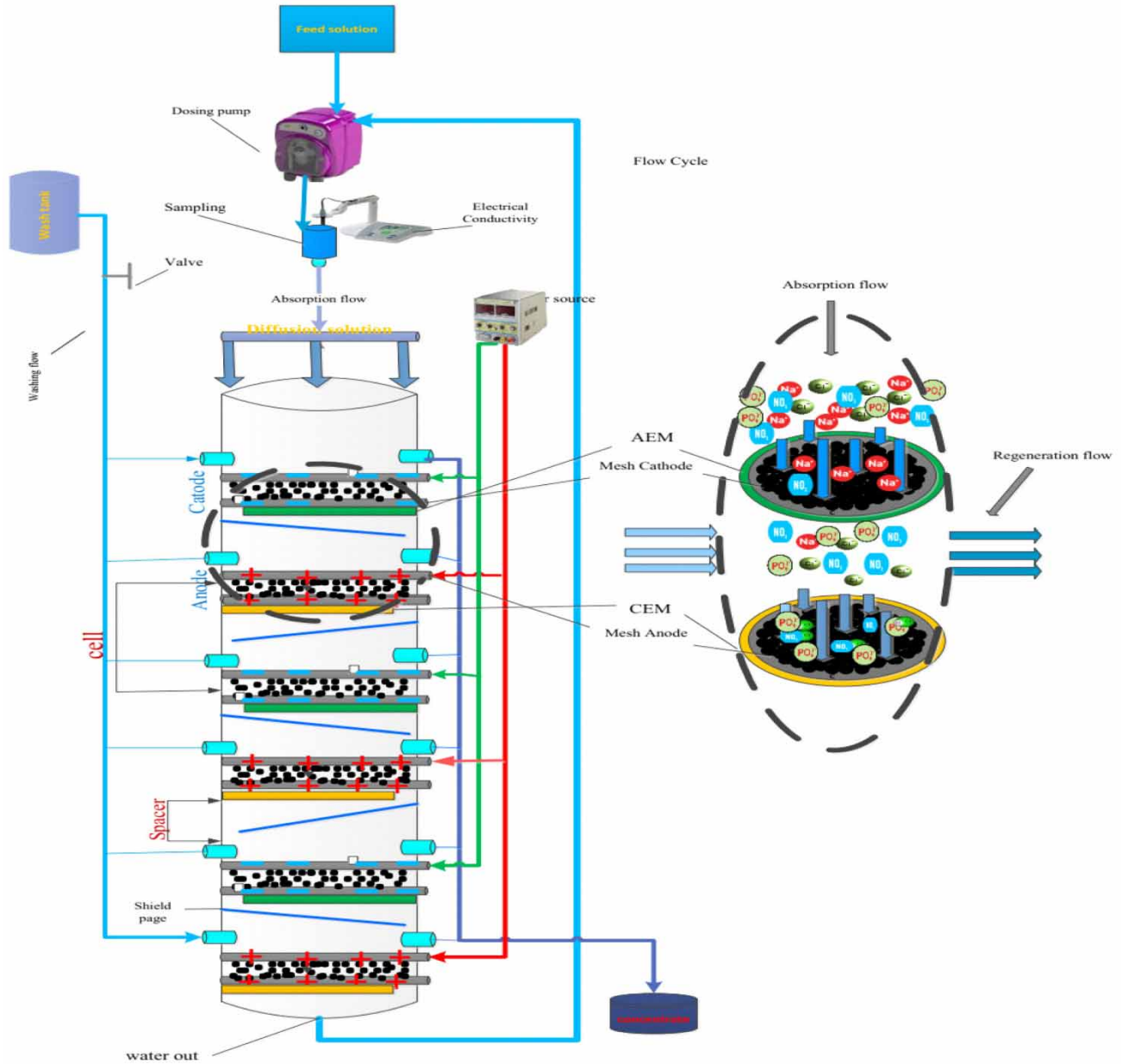
Figure 3 | Schematic diagram of the experimental set-up.

(1)), adsorption capacity (Equation (2)), and specific energy consumption (SEC) (Equation (3)).

$$RE(\%) = \frac{C_0 - C_e}{C_0} \times 100 \tag{1}$$

$$RE(\%) = \frac{(C_0 - C_e)V}{M} \tag{2}$$

$$SEC = \frac{1000E}{M.Q} \tag{3}$$

where, C_0 and C_e are the initial and final ion concentrations in solution (mg/L or μc/cm), respectively. V is the volume of the solution, M is the adsorbent mass (g/L), q_e is the specific adsorption capacity of the electrodes (mg/g), and SEC (wh/g) is specific energy consumption. In Equation (3), E (Wh) is energy consumed (Zhao *et al.* 2013).

2.4. Electrode material characterization

Morphology, composition, and surface functional groups of carbon aerogel electrodes made using electron microscopy (Sarrafi *et al.* 2016) (Hitachi, S-4800), Raman spectroscopy (Horiba Jobin Yvon, Labram HR), and infrared spectroscopy (FTIR, Bruker Vertex 70), were determined, respectively. In addition, the surface properties of the electrode materials were estimated using Brunauer–Emmett–Teller (BET) analysis using N_2 adsorption isotherms at 77 K (Tristar II Plus, Micrometrics). For this analysis, the samples were degassed using N_2 gas at 145 °C overnight before determining their concentration. The concentration of sodium and calcium chloride ions were determined by electric conductivity meter. Also, the concentration of nitrate and phosphate ions were determined according to the Standard Methods for the Examination of Water and Wastewater using codes 4,500 and 4,110, respectively (APHA 2012).

3. RESULTS AND DISCUSSION

3.1. Characterization of electrodes

Field emission scanning electron microscope (FESEM) was applied to study the morphology of samples (Rasoulzadeh *et al.* 2021a, 2021b, 2021c). Figure 4(a) (I, II, and III) displays FESEM images of the pristine aerogel carbon beads. Figure 4(b) (IV, V and VI) displays FESEM images of exhausted aerogel carbon particles. Pristine aerogel carbon displays non-sphere morphology with porous structure. In addition, compared with pristine aerogel carbon, as clearly observed in Figure 4 (IV, V and VI). Based on Figure 4 (before and after using the process) and considering the erosion and deformation that it shows after use, it can be concluded that the process of adsorption of ions from the solution is well formed.

To demonstrate the elemental compositions of materials prior and post operation, EDX was used (Gholami *et al.* 2020; Rasoulzadeh *et al.* 2021a, 2021b, 2021c). Figure 4(b) (I and II) presents the EDX spectrum of the samples. As can be seen in Figure 5(b), the peaks observed in native aerogel carbon were, also, observed in utilized aerogel carbon except some peaks appeared at 0.28, 1.2, 2.1, 2.62, and 3.7 keV which are association with adsorbed ions.

Figure 4(c) shows the Raman spectra of this electrode material. This spectra displays presence of two strong bands at 1,450 cm^{-1} and 1,500 cm^{-1} which assign to the D and G bonds and belong to the disordered carbon atoms in its amorphous phase.

BET analysis and BJH isotherm using N_2 adsorption/desorption were used to determine the specific surface area and pore size of aerogel carbon nanoparticles (Alipour *et al.* 2021; Rasoulzadeh *et al.* 2021a, 2021b, 2021c). N_2-sorption isotherms of aerogel carbon are shown in Figure 4(d) (I and II). According to BET, the specific surface area and the pore volume of the sample were found to be 489 m^2/g and 0.3041 cm^3/g, respectively. Furthermore, its average particle diameter was obtained as 158.85 nm.

3.2. Determining the optimal FTCDI conditions

3.2.1. Effect of voltage on sodium chloride removal efficiency

One of the most important parameters in the amount of adsorption of soluble ions by various CDI cellular structures is the electrical potential. The effect of the applied voltage on the electrosorption performance is illustrated in Figure 5. Different values of the applied voltage from 0, 0.8, 1 to 1.2 V were tested. As shown in Figure 5, the amount of sodium chloride absorbed increases by increasing voltage range from 0 to 1.2 V. When voltage is not applied (V = 0), only physical adsorption occurs in the system, so that the slope of physical adsorption decreases over a period of 10 min. After the saturation of surface pores, the electrodes will no longer be absorbed during this time and the system will reach saturation. However, by applying a voltage from 0.8 to 1.2 V, in addition to physical adsorption, electrochemical adsorption is also performed. The removal efficiency of sodium chloride (Equation (1)) using voltages of 0, 0.8, 1, and 1.2 V becomes 13, 33, 40.5, and 54.5%, respectively. This type of adsorption, electrochemical adsorption, will cause all the double electrode layers and the electrode pores to be involved in the adsorption process. Thus, the saturation time of the electrode pores will be longer and more ions will accumulate in the double electrode layers. In general, it can be concluded that the effect of voltage on the rate of sodium chloride adsorption is directly related to aerogel carbon electrodes. The study of Xing *et al.* (2019) shows that there is a direct relationship between the amount of potential difference applied to carbon electrodes and the rate of adsorption of accumulated sodium chloride ions. Hence, by applying voltages of 0.6, 0.9, and 1.2 V, the removal efficiency was 6.4, 18, and 32%, respectively (Xing *et al.* 2019). Also,
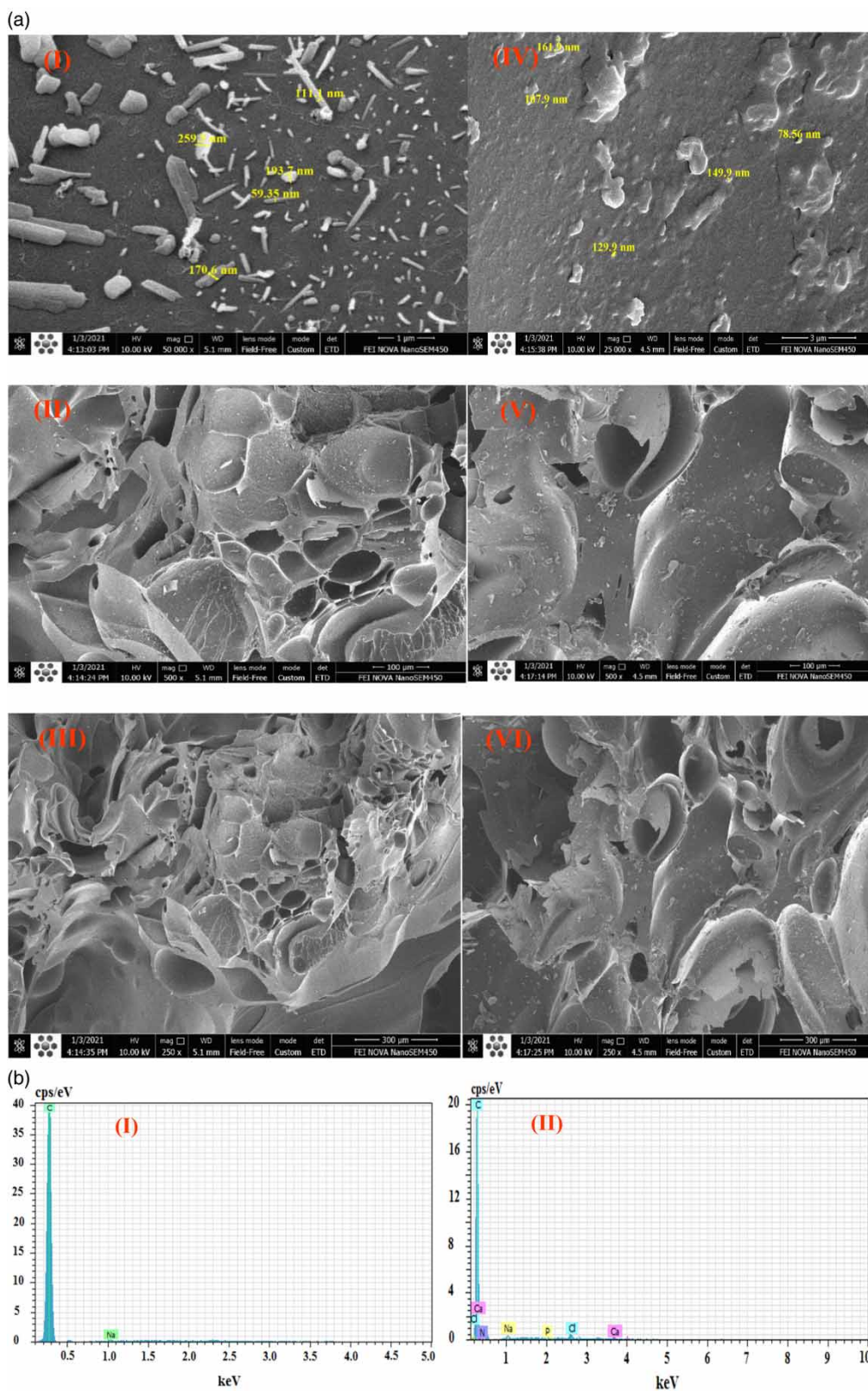
Figure 4 | Characterization of materials: (a) FESEM images I, II, III are related to the fresh aerogel carbon and IV, V, VI are related to the exhausted aerogel carbon; (b) EDX spectrum I belongs to the fresh aerogel carbon and II belongs to the exhausted aerogel carbon; (c) Raman spectra; and (d) N_2-sorption isotherm I and BJH pore size distribution II. (*continued*.).

Date:1/4/2021 5:41:44 PM HV:25.0kV Puls th.:4.11kcps

El AN Series unn. C norm. C Atom. C Error (1 Sigma)
[wt.%] [wt.%] [at.%]   [wt.%]

C 6 K-series 99.85 99.85 99.92   12.38
Na 11 K-series 0.15   0.15   0.08   0.05

Total: 100.00 100.00 100.00

Date:1/4/2021 5:42:18 P MHV:25.0kV Puls th.:2.49kcps

El AN Series unn. C norm. C Atom. C Error (1 Sigma)
[wt.%] [wt.%] [at.%]   [wt.%]

C 6 K-series 95.01 95.01 96.21   12.07
N 7 K-series   3.78   3.78   3.28   2.08
Cl 17 K-series   0.54   0.54   0.19   0.06
Na 11 K-series   0.53   0.53   0.28   0.08
Ca 20 K-series   0.14   0.14   0.04   0.04
P 15 K-series   0.03

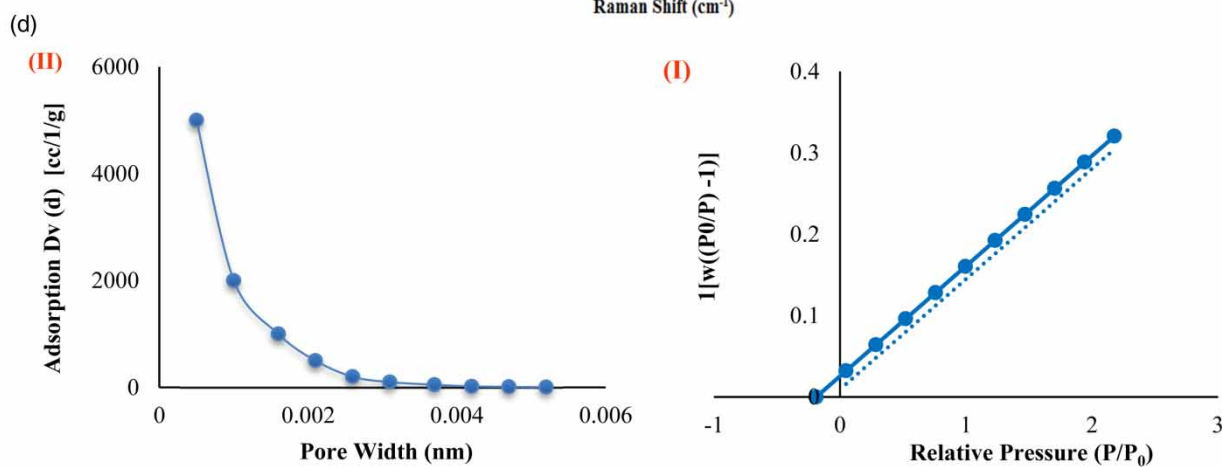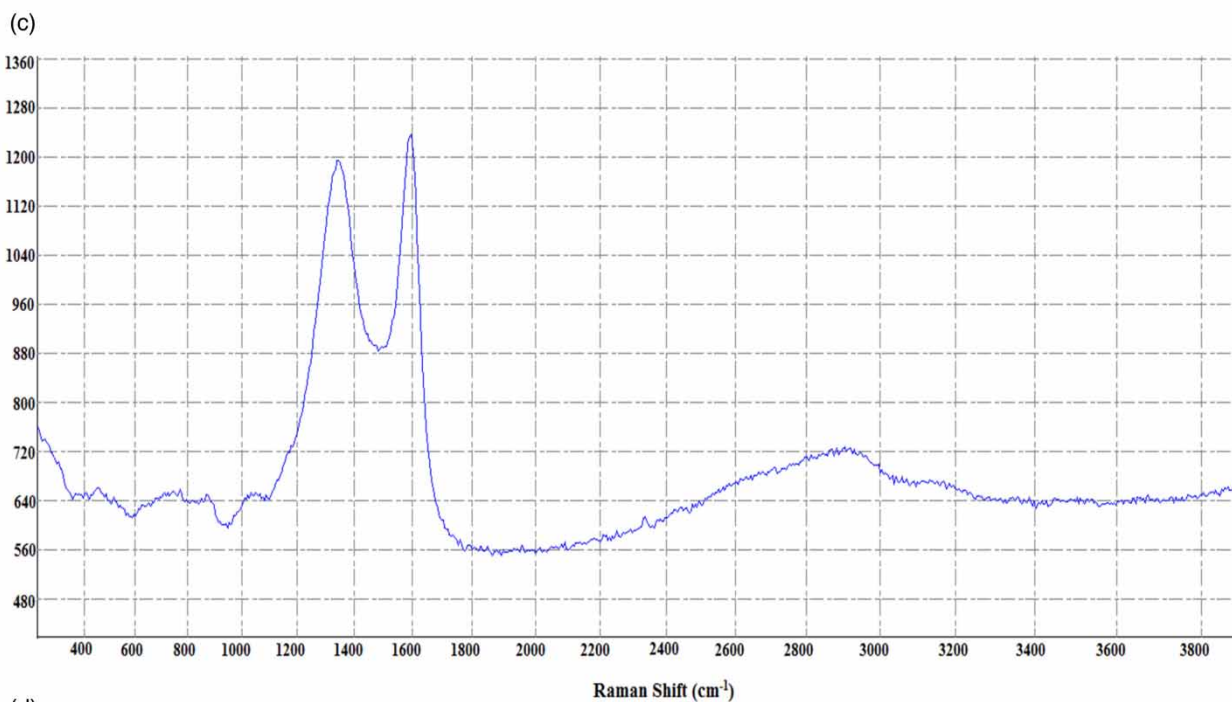Total: 100.00 100.00 100.00

(c)

(d)

Figure 4 | Continued.

Mossad & Zou (2013) reported that as the voltage increases, more salt concentrations from aqueous solutions are absorbed by the system, so that at voltages of 0.6, 0.8, 1, and 1.2 V, the removal efficiencies were 51, 53, 57, and 61%, respectively.
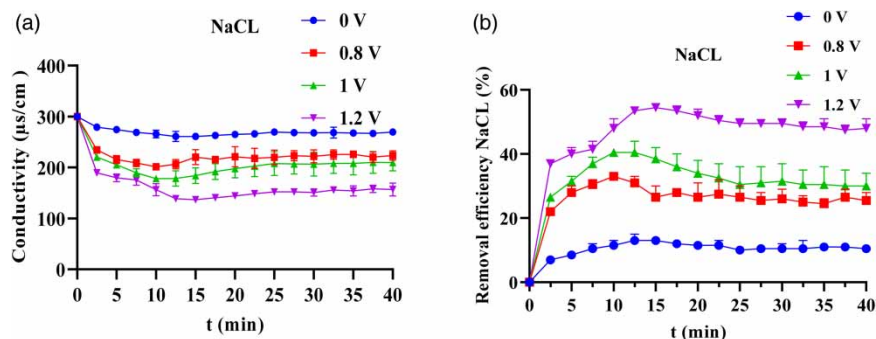
Figure 5 | (a) The effect of different voltages on the electrochemical adsorption process of sodium chloride. (b) Sodium chloride removal efficiency in the presence of an initial concentration of 300 μs/cm, a flow rate of 40 mL/min, and a carbon particle diameter between 0.9 and 1 mm.

3.2.2. Effect of input flow rate on sodium chloride removal efficiency

Another parameter affecting the performance of the FTCDI system was the change in input velocity to the system. By changing the flow velocity, the contact time, the probability of collision, and adsorption change between the electrodes and the soluble ions. Therefore, it is necessary to determine the relationship between the flow velocity and the amount of ions removed from the solution. Figure 6(a) and 6(b) show the effect of different flow rates on the electrochemical adsorption process of sodium chloride and the removal efficiency of sodium chloride in the presence of an initial concentration. According to Figure 6(a), under constant conditions with a voltage of 1.2 V, electrical conductivity (EC) of 300 μs/cm and a diameter of carbon particles of 0.1–0.9 mm, the amount of absorbed salt also increased with increasing flow velocity. The reason for this is that the FTCDI system is a closed and circulating system, since the hydraulic retention time (HRT) of the system is inversely related to the velocity. According to Equation (4), it could be that if the flow velocity increases, the number of cycles or circulations of the solution in a time interval in the system increases. Finally, by increasing the number of cycles in a period of time, the probability of contact and dissolution of soluble ions with the electrode will increase. In flow velocity of 40, 60, and 80 mL/min, the adsorption efficiency obtained was 54.5, 63, and 69%, respectively. The results of a study by Xing *et al.* (2019) show that under constant conditions, with increasing flow velocity of 20, 32, and 44 mL/min, the effluent concentration decreases. In other words, by increasing flow velocity, the amount of adsorbed salt decreases. Pastushok *et al.* (2019) reported that the amount of salt absorbed increases as the flow velocity decreases. However, it should be noted that in the studies mentioned, the changes of flow velocity on the removal efficiency have been investigated in only one cycle, and that is why reducing the flow velocity increases the efficiency.

$$\emptyset = \frac{v}{t} \Rightarrow t = \frac{v}{\emptyset} \tag{4}$$
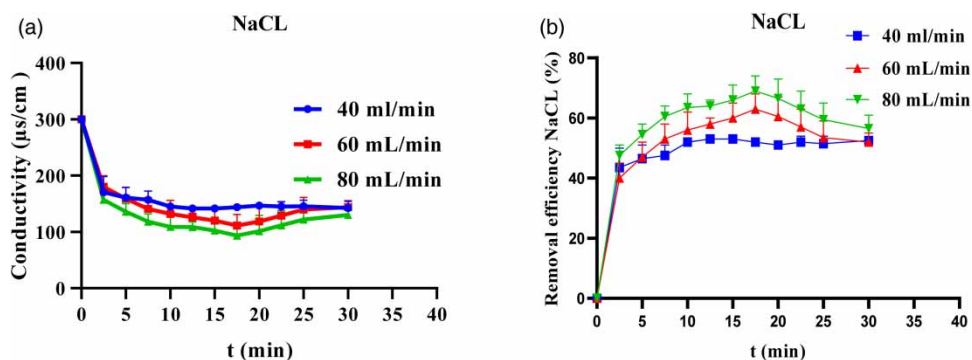
$$n = \frac{\emptyset}{t} \tag{5}$$

Figure 6 | (a) The effect of different flow rates on the electrochemical adsorption process of sodium chloride. (b) The removal efficiency of sodium chloride in the presence of an initial concentration of 300 μs/cm, voltage 1.2 V, and carbon particle diameter between 0.9 and 1 mm.

where, $\varnothing$ is the flow velocity (mL/min), t is the hydraulic retention time (min), v is the sample volume (mL), and n is the number of cycles.

3.2.3. Effect of aerogel carbon particle diameter on sodium chloride removal efficiency

Depending on the cellular structure of each CDI system, the way the adsorbent is used is different. For example, in conventional flow by CDI and MCDI, the used adsorbent is attached to the electrode surface in the form of a layer with a certain thickness, or in the FCDI system, the adsorbent is used as a slurry in the chamber. In the present study, aerogel carbon used in the form of granules was placed between the two mesh plates of each electrode to allow the flow of solution to pass through the electrode (Figure 2(b)). The flow rates, contact time, and the probability of collision between carbon pores and soluble ions are effective parameters in increasing the efficiency of the system. In other words, the size of the granules is significantly related to them, so it is necessary that the effect of diameter changes on performance. Figure 7(a) and 7(b) show the effect of different diameters of aerogel carbon granules on the electrochemical adsorption process of sodium chloride and the removal efficiency of sodium chloride, respectively. As shown in Figure 7, there is an inverse relationship between granule diameter and system efficiency. In constant conditions, with increasing the diameter from 0.9, 1–2, and 2–3 mm, the removal efficiency decreased by 69, 52, and 46%, respectively. The reason for this decrease can be due to the increase in the diameter of the grains, because as the diameter increases, the density of the granules decreases and the distance between them increases. It is at this point that the ions pass more easily and with less contact with the granules and, finally, the efficiency of the system decreases with increasing diameter of the granules. To increase the efficiency, the diameter of the grains cannot be significantly reduced, because in these conditions, a drop in water pressure occurs. The findings of Bian *et al.* (2019) show that by reducing the diameter of carbon particles from 2–5 mm to 0.4–8 mm, salt adsorption efficiency increases.

3.2.4. The effect of different concentrations on the removal efficiency of sodium chloride

The performance of a CDI system is affected by changes in the input concentration. The experiments were performed under optimal conditions. Removal efficiency and adsorption capacity for concentrations of 150, 300, and 450 mg/L were 75.5%, 82.5%, and 82.5%, respectively. Also, adsorption capacity for concentrations of 150, 300, and 450 mg/L were 15.45, 33, and 55.68 mg/m, respectively. Figure 8(a) and 8(b) show the effect of different concentrations of sodium chloride on the electrochemical adsorption process and the removal efficiency of sodium chloride in the presence of optimal voltage conditions, respectively. According to Figure 8(a), the results show that the removal efficiency increases with increasing concentration of the solution. By increasing salinity, the ionic resistance of the solution decreases and, as a result, the efficiency increases (Yeo & Choi 2013). As the concentration of ions in the solution increases, the conductivity of the solution increases and causes the electrode to access the ions with less electrical resistance. However, some studies have shown that the effluent concentration increases with increasing inlet concentration, due to the rapid saturation of the double electric layers (Huyskens *et al.* 2013; Jiang *et al.* 2018). The reason for such a discrepancy can be explained by the difference in the range of concentrations of the solution used. According to Figure 8(b), the ion adsorption rate decreases over time. The maximum amount of adsorption was observed in 20 min. After that, the adsorption process is almost stopped, which indicates the saturation time of the electrodes. Electrode placement can be described as the solution flow will cause the adsorbed ions to
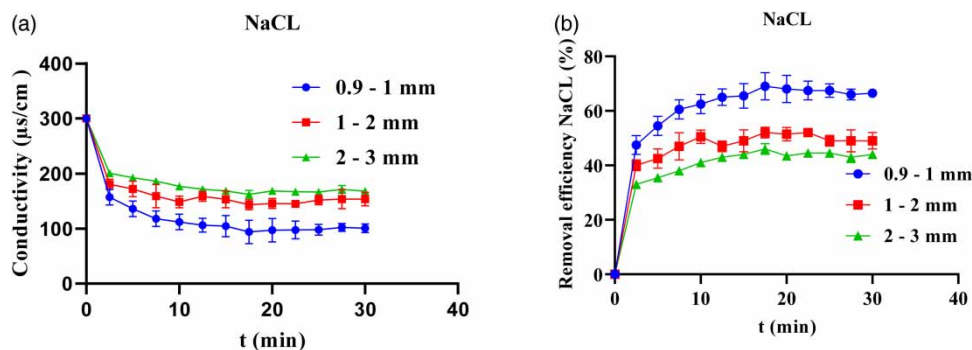

Figure 7 | (a) The effect of different diameters of aerogel carbon granules on the electrochemical adsorption process of sodium chloride. (b) The removal efficiency of sodium chloride in the presence of voltage 1.2 V, flow rate 80 mL/min, 300 µs/cm.
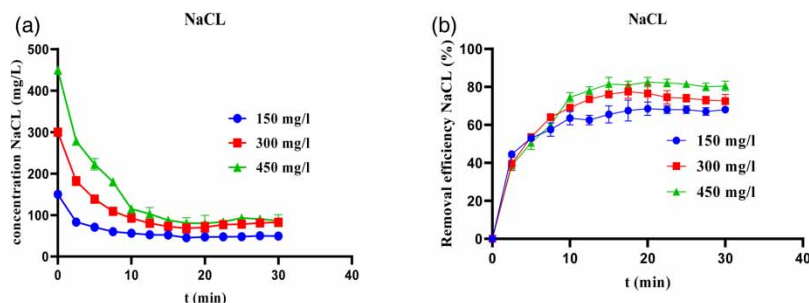
Figure 8 | (a) The effect of different concentrations of sodium chloride on the electrochemical adsorption process. (b) The removal efficiency of sodium chloride in the presence of optimal voltage conditions of 1.2 V, flow rate 80 mL/min, and carbon particle diameter between 0.9 and 1 mm.

separate again from the electrode and enter the effluent, thus reducing system performance after saturation time. The study of Chang et al. (2020) shows that by increasing the input concentration from 250 to 1,000 mg/L, the removal efficiency increases. Tang et al. (2015) reported that with increasing input concentration, the removal efficiency increases so that the adsorption rate in the initial times is much higher than the final times. Wang et al. (2015) reported that system efficiency decreases with increasing input concentration.

3.3. System performance in removing other pollutants

3.3.1. Calcium chloride adsorption efficiency

Calcium chloride is one of the effective ions in the salinity of solutions, so it is necessary to know how much success the system can have in reducing its concentration. As shown in Figure 9, the maximum removal efficiency was 49% and the maximum adsorption capacity was 33.15 mg/g in 15–20 min. Then, the amount of salt absorbed decreases as the carbon pores become saturated. The slope of the adsorption efficiency up to 10 min indicated that the adsorption efficiency speed was much higher during this time. It can be justified in two ways. First, the concentration of the solution is still high during this period, according to the cases mentioned earlier, the electrical resistance is low. Second, the pores of the carbon electrodes are not yet fully saturated, thus, the adsorption rate will be faster than the remaining time. The optimal conditions for determining the adsorption efficiency of calcium chloride were similar to sodium chloride. It is observed that sodium chloride at a concentration of 450 mg/L, adsorption efficiency was 82.5% but for calcium chloride was 49%. Due to the use of various samples and high concentrations as well as the repetition of experiments, over time, the absorption or removal capacity of the system decreases compared to the initial time of the system. Hou & Huang (2013) reported that the amount of calcium chloride absorbed was less than sodium chloride. Hassanvand et al. (2018) reported that calcium chloride adsorption efficiencies are lower than sodium chloride.
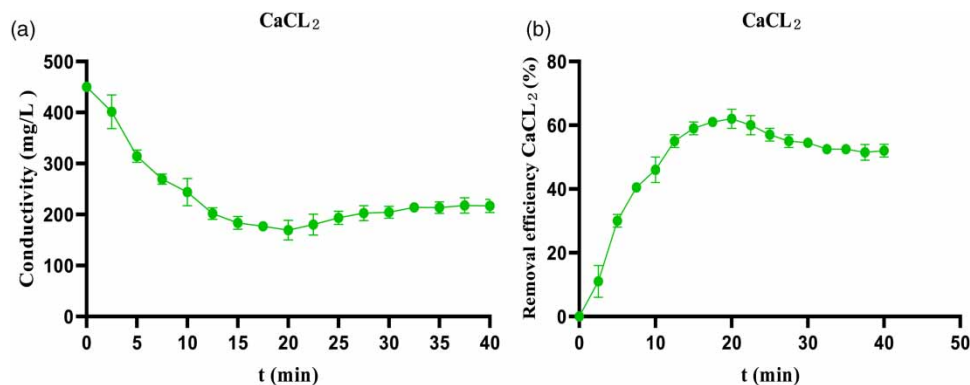

Figure 9 | (a) Determination of electrochemical absorption of calcium chloride with a concentration of 450 mg/L. (b) Calcium chloride removal efficiency in the presence of optimal voltage conditions of 1.2 V, 80 mL/min flow, and carbon particle diameter between 0.9 and 1 mm.

3.3.2. Nitrate removal from the synthetic samples

The performance of the system was tested in electrochemical adsorption of nitrate under conditions of 2 V, 80 mL/min, and carbon diameter of 0.9–1 mm with different concentrations of 30, 50, and 70 mg/L. In this experiment, similar to in Section 3.2.4, the efficiency increases with increasing initial concentration. Figure 10(a) and 10(b) presents the effect of different concentrations of nitrate on the process of electrochemical adsorption and nitrate removal efficiency in the presence of optimal voltage conditions, respectively. According to Figure 10(a), the maximum removal efficiencies were 74, 79, and 85%, respectively. Also, the maximum adsorption capacity of each electrode was 3.15, 5.85, and 8.85 mg/g. The aim of this study was to reduce the nitrate concentration to below its standard level set by WHO and EPA (50 mg/L and 45 mg/L, respectively) in drinking water. Based on this study, it can be concluded that the designed system is able to reduce the nitrate concentration to the desired level. Depending on the concentration of nitrate in the water to be treated, any amount of soluble nitrate can be reduced to less than the standard by increasing the number of electrodes and thus increasing the adsorption capacity of the system. Uzun & Debik (2019) reported that the CDI system can reduce the concentration of soluble nitrate in water resources (river) at a lower cost than other methods (Uzun & Debik 2019). Tang *et al.* (2015) reported that under different conditions and with the presence of other cations and anions, CDI systems could be used to significantly reduce nitrate concentrations.

3.3.3. Removal of phosphate from the synthetic samples

According to EPA standards, the maximum concentration of phosphate ions in drinking water is less than 0.03 mg/L. Based on this value, performance of the system was tested at different initial concentrations (1, 2, and 3 mg/L) and under constant conditions with a flow rate of 80 mL/min, voltage of 2 V, and carbon diameter of 0.9–1 mm. As can be seen from Figure 11, the system has a good performance in removing the system in 40 min. At concentrations of 1, 2, and 3 mg/L, the removal efficiencies were 77, 87, and 90%, respectively. Adsorption capacity, also, was 0.108, 0.225, and 0.39 mg/g, decreasing or increasing the phosphate concentration in solution depends on the pH. Therefore, its solution pH was adjusted close to the drinking water pH so that the system would not be too affected by temperature changes. Findings of a study by Bian *et al.* (2019) showed that the maximum removal efficiency of phosphate of 83% was reported after 7 h.

3.4. Real samples: faucet water

Ramhormoz city is one of the cities of Khuzestan province in Iran, which is located in the northeast of the province and situated in the Khuzestan plain at an altitude of 179 meters above sea level (Khavarian-Garmsir *et al.* 2019). The sources of drinking water supply in this city are rivers and deep wells. Unfortunately, due to the TDS and the high total hardness, its consumption is impossible for the general population of the city, so that the people spend a lot of money on their drinking water every year (Abtahi *et al.* 2015). Therefore, to determine the physicochemical characteristics of the city's water and also to evaluate the ability of the system to deionize this type of water resource, sampling was performed from three points, and the
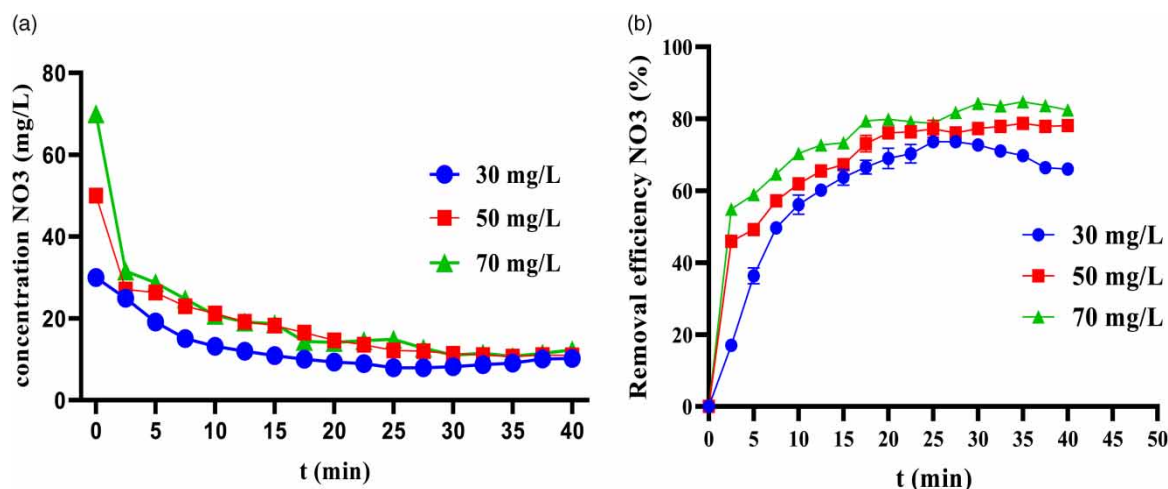

Figure 10 | (a) The effect of different concentrations of nitrate on the process of electrochemical adsorption. (b) Nitrate removal efficiency in the presence of optimal voltage conditions of 2 V, 80 mL/min, and carbon particle diameter between 0.9 and 1 mm.
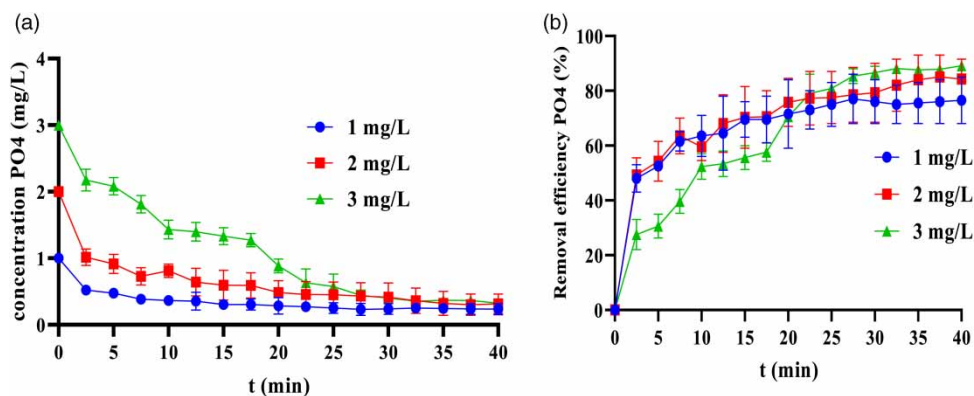
Figure 11 | (a) The effect of different concentrations of phosphate on the electrochemical adsorption process. (b) Phosphate removal efficiency in the presence of optimal voltage conditions of 2 V, 80 mL/min, and carbon particle diameter between 0.9 and 1 mm.

samples were collected and transferred to the water and wastewater laboratory. After determining the physicochemical characteristics (pH, TDS, turbidity, electrical conductivity, hardness, chlorine, nitrate, and phosphate) of the samples taken, process efficiency was evaluated to remove contaminants.

After determining the physicochemical characteristics of samples taken, a volume of 150 mL from each sample was injected into the system. In this stage, the conditions applied to the system were similar to the ones during the treatment of NaCl (flow rate: 80 mL/min, voltage: 1.2 V, carbon aerogels diameter: 0.9–1 mm).

To further reduce the salinity of water, this condition were selected. In this study, the final goal was to use this system in real conditions, thus, the voltage selected should have the least effect on causing Faradaic reactions and oxidation of electrodes. The voltage 1.2 V, also, achieved an acceptable efficiency in the removal of nitrate and phosphate.

The performance of a water treatment system in the face of water resources is different from synthetic samples that have only one type of ion. Because the interaction of other ions with each other in real samples may increase or decrease the efficiency of the system, the ultimate goal was to use the CDI system in the purification and desalination of real samples. In this study, the water resources of Ramhormoz city were used, because their water resources contain high salts. Table 1 summarizes the water features of this city. Based on Table 1, TDS, EC, hardness, chlorine, and turbidity are much higher than the standard. According to Table 2, it can be seen that the system has a removal efficiency of 54.4% nitrate, 66.6% phosphate, 36.5% chlorine, and 33.3% total hardness and finally reduced them to less than the standard level. However, in terms of reducing the concentration of TDS, EC, and turbidity, despite a decrease of 23.5, 39 and 25%, respectively (TDS absorption capacity 60 mg/g) the levels are still higher than the standard. Therefore, it was concluded that this pilot was not able to reduce TDS and EC to the desired level. The reason for such performance against high concentrations of TDS and EC can be attributed to the low number of electrodes. Owing to the limited adsorption capacity of the electrodes, more carbon and electrodes are needed to further reduce the concentration. In this case, with increasing the number of electrodes and, finally, the amount of carbon, the adsorption capacity of the system increases and its saturation time will be longer. Therefore, it can be expected that this system will be able to place a higher concentration of soluble solutes between its pores. Thanks to repeated experiments during the study (more than three months of continuous testing with different concentrations), the adsorption capacity of the electrodes has decreased compared to the starting time. Therefore, it is not possible to expect the EC and TDS to fall below the desired level. A study was conducted by Lee *et al.* (2019) for desalination of domestic wastewater. The results show that the MCDI pilot under conditions of 1.2 V and flow rate of 10 mL/min in contact with the synthetic sample of sodium chloride with an initial concentration of 1,200 μs/cm at the duration of 180 min decreased to less than 1.27 μs/cm (more than 99% efficiency). However, in contact with domestic wastewater containing TDS of 276.7 mg/L, EC 437 μs/cm (much less than the actual sample in the present study), turbidity 0.27 NTU, hardness 118.2 mg/L, nitrate 57 mg/L

Table 1 | Summary of water status of Ramhormoz city

pH	Turbidity (NTU)	TDS (mg/L)	Hardness (mg/L)	Chlorine (mg/L)	Phosphate (mg/L)	Nitrate (mg/L)	Electrical conductivity (μs/cm)	Temperature (°C)
7.4	12	1,700	540	550	0.09	28.8	3,480	23.2

Table 2 | A summary of the performance of the system in the water treatment of Ramhormoz city

Property	Entrance	Output	Permissible and desirable limit based on Iranian drinking water standard 1053	Removal efficiency (%)	Adsorption capacity (mg/g)
pH	7.4	7.2	6.5–8.5	–	–
Turbidity (NTU)	12	9	1–5	25	
TDS (mg/L)	1,700	1,300	1,000–1,500	23.5	60
Hardness (mg/L)	540	360	500–200	33.3	27
Chlorine (mg/L)	550	349	400–250	36.5	30.15
Phosphate (mg/L)	0.09	0.03	0.08–0.03	66.6	0.009
Nitrate (mg/L)	28.8	14	50	54.4	2.2
EC (μs/cm)	3,480	2,119	1,500–800	39.1	–
Temperature (°C)	23.2	24	–	–	–

and phosphate 11.6 mg/L the efficiency reduced to 48.6 mg/L, 99.1 μs/cm, 0.20 NTU, 9.3 mg/L, 5.9 mg/L, and 8/7 mg/L, respectively. The reason for such a decrease in efficiency compared to the synthetic state is the existence of interactions of other ions, including calcium, magnesium, sodium, potassium, sulfate, carbonate, nitrate, and phosphate (Lee *et al.* 2019). Also, a study conducted by Jiang *et al.* (2019) to remove phosphate from domestic wastewater using a conventional MCDI system showed that only the maximum efficiency of 57% was reached under conditions with voltage of 1.2 V, flow rate of 24 mL/min, and pH = 7.2. If, as in the present study, this efficiency has reached 66.6%, the reason for such an increase in efficiency compared to the Jiang *et al.* (2019) study, can be described because of the modified system compared to the conventional MCDI and the type of sample used. On the other hand, the previous studies have shown that the transfer of different ions under the same conditions from the solution to the electrodes and their adsorption can be different. Ions with smaller hydrated radii move faster towards the electrodes. On the other hand, high ion capacity is also important to remove more ions (Liang *et al.* 2013). Four studies have emphasized that monovalent ions are more efficiently adsorbed than divalent ions (Johnson & Newman 1971; Gabelich *et al.* 2002; Xu *et al.* 2008; Martínez-Landeros *et al.* 2019). The reason for this result in those studies is that the pore size of their electrodes varies from micropores (<2 nm) to mesopores (2–50 nm). This distribution of pore sizes causes ions to have very different tendencies to be absorbed by an electrode (Seo *et al.* 2010). As a result, the reason for the removal of more monovalent ions than divalent ions is the fact that divalent ions have a hydrated diameter between 6 and 7 Å.

Monovalent ions have a considerably lower hydrated diameter (4 Å) compared to the multivalent ions (6–7 Å). Therefore, electrode pores are occupied with monovalent ions in a higher rate than multivalent ions. This leads to the lower adsorption of multivalent ions. However, in our study, different results were obtained, so that under the same conditions (80 mL/min, 1.2 V, and 1.9 mm), the removal efficiency of PO_4^{3-} ion compared to NO_3^- ion and nitrate ion compared to ion Cl^- is higher. This discrepancy can be seen in the size of the pores of the electrodes, since the carbons are concentrated in the form of granules in the electrode and a great deal of porosity is obtained. There is no competition between ions with low or high hydrated radius. Phosphate and nitrate tends to be more adsorbed by the electrodes due to their higher charge capacity. These results are consistent with studies by Fan *et al.* (2016), Kim *et al.* (2013), and Uzun & Debik (2019), because they also emphasized that the adsorption efficiency of nitrate, phosphate, and sulfate ions was higher than that of chloride and fluoride ions under constant conditions. Therefore, it can be concluded from the above that the removal of less salinity than the removal of phosphate and nitrate is somewhat justifiable.

3.5. Cost assessments and comparisons

Calculation of adsorption capacity and comparison between them can be carried out using the following equations. The method of calculating the adsorption capacity (Q_{ads}) and specific energy consumption (SEC) in the FTCDI in comparison with the conventional MCDI is presented in Equations (6) and (7), respectively (Zhao *et al.* 2013):

$$Q_{ads} = \frac{(C_i - C_f)V}{M} \tag{6}$$

$$SEC = \frac{1000E}{m.Q_{ads}} \tag{7}$$

where, C_i and C_f (mg/L) indicate the initial and final (equilibrium) concentrations of the inlet stream, respectively; V (L) is the volume of solution applied in the system; M (g) represents the mass of aerogel carbon granules on the mesh electrode; E (Wh) and Q_{ads} (mg/g) are the energy consumption and adsorption capacity in the FTCDI system, respectively.

The cost analysis, in terms of capacity adsorption and energy consumption of the FTCDI system, at working voltage of 1.2 V for different pollutants is shown in Table 3. Based on Table 3, the presence of sodium and calcium ions in the solution reduces the energy consumption of the FTCDI system because they have a higher adsorption capacity than nitrate and phosphate. The maximum consumption energy of FTCDI was nearly 276.92 Wh/g for nitrate which was 138 and 70 times sodium and calcium, respectively. It is concluded that the FTCDI tends to adsorb sodium and calcium more than nitrate. On the other hand, the FTCDI has high selectivity for sodium and calcium. Table 4 shows comparison of adsorption performance of different pollutants using aerogel carbon granules containing mesh electrode. Based on Table 4, the FTCDI shows the good efficiency in NaCl removal with reasonable consumption of energy.

3.6. Regeneration studies

The performance of the spent carbon aerogel regeneration experiment was studied using the FTCDI system with optimum result (voltage 1.2 V, carbon particle diameter between 0.9–1 mm, and flow rate 80 mL/min). After each adsorption test, the adsorption flow valves close and the flushing flow opens at the same time as the voltage is reversed. Then, the ions adsorbed were desorbed by injecting 0.24 mL/s distilled water (0 μs/cm) to the column for 5–10 min until the EC of distilled water attained the removed EC in the adsorption phase. Subsequently, the next adsorption experiment started. The mentioned cycle was repeated for ten series. The system removal efficiency for the first experiment was 92.1% and the tenth experiment showed a removal efficiency of 88.3%. Therefore, the obtained sorbents can lose up to ~4% of their removal efficiency of the first cycle after ten experiments. On this basis, carbon aerogel was found to be a stable material as FTCDI electrode and can be reused multiple times with good performance. This confirms a significant balance between its affordability and its ecological impact.

Table 3 | Energy consumption at working voltage of 1.2 V for adsorption of different pollutants

Pollutant	Adsorption capacity (mg/g)	Energy consumption (Wh/g)	Cost ($/g of carbon)
Sodium chloride	55.68	1.94	0.0057
Calcium chloride	33.15	3.26	0.0096
Nitrate	5.85	276.92	0.82
Phosphate	0.39	18.46	0.052
TDS	60	1.80	0.0053

Table 4 | Comparison of adsorption performance of different pollutants using aerogel carbon granules containing mesh electrode

Type of system	Material	Applied voltage (V)	Flow rate (mL/min)	Type of pollutant (input concentration)	Duration of adsorption process (min)	Energy consumption	Adsorption capacity (mg/g)	Removal efficiency (%)	Reference
CDI	Activate carbon	1.8	5	NaCl (12 μs/cm)	66	–	1	74%	Sufiani et al. (2020)
MCDI	Activate carbon	1.2	10	NaCl (10 mM)	48	120 (Wh/m^3)	9.07	65%	Lee et al. (2019)
FTCDI	Activate carbon	1.2	2	Nitrate (70 mg/L)	25	–	5.5	48%	Pastushok et al. (2019)
FTCDI	Carbon aerogel	1.2	80	TDS (1,700 mg/L)	40	1.8 (Wh/g)	60	23%	Present study
FTCDI	Carbon aerogel	1.2	80	NaCl (450 mg/L)	40	1.9 (Wh/g)	55.68	82.5%	Present study
FTCDI	Carbon aerogel	1.2	80	Nitrate (70 mg/L)	40	276 (Wh/g)	5.8	85%	Present study
FTCDI	Carbon aerogel	1.2	80	Phosphate (3 mg/L)	40	18 (Wh/g)	0.39	90%	Present study

4. CONCLUSIONS

CDI is an electrochemical technology which uses electric fields between two electrodes to temporarily remove ionic species from water. Excess ions in water and wastewater include a variety of salts (sodium, calcium chloride, etc.), nitrates, phosphates, sulfates, heavy metals, colloids, organic compounds, biomolecules, and a variety of bacteria and viruses. Other important ions can also be removed and placed in porous electrodes as long as these materials are stored in the pores of the used electrodes. Based on the results obtained and comparing them with other studies, the MCDI system has been modified, in which permeable mesh electrodes enable the solution current to pass through the electrode itself and ultimately increase the level of contact of ions with carbon and use the maximum capacity ($2,934 \, m^2/g$). In synthetic solutions, sodium chloride (82.5%), calcium chloride (49%), nitrate (85%), and phosphate (90%) can be removed. Also, in contact with the real sample the following were reduced: turbidity (25%), total hardness (33.3%), phosphate (66.6%), nitrate (51.4%), electrical conductivity (29%), and total solids (11.8%). Therefore, if the general purpose of using this process is to remove high concentrations of ions from water sources, it is necessary that the number of electrodes and the amount of adsorbent for this system are designed and set up properly, then it is possible to remove target pollutants with high efficiency by consuming low energy. Such a system will be able to remove any concentration from solutions with very low energy consumption and high efficiency.

4.1. Suggestions

Based on the results of the findings of this study, these cases can also be considered for future studies:

- The synthesis of an adsorbent with low electrical resistance, high specific surface area, and oxidation resistance to enable the process to perform better and more efficiently.
- In the case of research in this field, first, determine the amount of adsorbent and the number of electrodes before starting the system by determining the amount of concentrations of contaminants under study and determining the area of the specific adsorbent surface. These items must be carefully checked before starting the system: absorbent dose required, number of electrodes used, concentration of target contaminant to be removed.
- Study the efficiency of the system in removing organic matter such as drugs, heavy metals, bacteria, and viruses.
- The operating time of the system and the adsorbent used, after which time the electrodes should be replaced, should be carefully calculated.
- Study of chemical and electrochemical reactions between adsorbent and adsorbed material.
- The possibility of exploitation at real scale and, finally, the possibility of its commercialization should be examined.

ACKNOWLEDGEMENTS

CONFLICTS OF COMPETING INTEREST

The authors declare that they have no known competing financial interests or personal relationships that could have appeared to influence the work reported in this paper.

DATA AVAILABILITY STATEMENT

All relevant data are included in the paper or its Supplementary Information.

REFERENCES

Abolhasani, S., Ahmadpour, A., Bastami, T. R. & Yaqubzadeh, A. 2019 Facile synthesis of mesoporous carbon aerogel for the removal of ibuprofen from aqueous solution by central composite experimental design (CCD). *Journal of Molecular Liquids* **281**, 261–268.

Abtahi, M., Golchinpour, N., Yaghmaeian, K., Rafiee, M., Jahangiri-rad, M., Keyani, A. & Saeedi, R. 2015 A modified drinking water quality index (DWQI) for assessing drinking source water quality in rural communities of Khuzestan Province, Iran. *Ecological Indicators* **53**, 283–291.

Algurainy, Y. & Call, D. F. 2020 Asymmetrical removal of sodium and chloride in flow-through capacitive deionization. *Water Research* **183**, 116044.

Alipour, M., Massoudinejad, M., Sanaei, D., Rasoulzadeh, H. & Hadei, M. 2021 Design and synthesis of two novel carbon aerogels using citric and tartaric acids as catalysts for continuous water desalination. *Desalination and Water Treatment* **215**, 69–79.

AlMarzooqi, F. A., Al Ghaferi, A. A., Saadat, I. & Hilal, N. 2014 Application of capacitive deionisation in water desalination: a review. *Desalination* **342**, 3–15.

Andelman, M. 2011 Flow through capacitor basics. *Separation and Purification Technology* **80** (2), 262–269.

APHA 2012 *Standard Methods for the Examination of Water and Wastewater*, Vol. 2. American Public Health Association, American Water Works Association, Water Pollution Control Federation and Water Environment Federation, Washington Dc, USA.

Baroud, T. N. & Giannelis, E. P. 2018 High salt capacity and high removal rate capacitive deionization enabled by hierarchical porous carbons. *Carbon* **139**, 614–625.

Bian, Y., Yang, X., Liang, P., Jiang, Y., Zhang, C. & Huang, X. 2015 Enhanced desalination performance of membrane capacitive deionization cells by packing the flow chamber with granular activated carbon. *Water Research* **85**, 371–376.

Bian, Y., Chen, X., Lu, L., Liang, P. & Ren, Z. J. 2019 Concurrent nitrogen and phosphorus recovery using flow-electrode capacitive deionization. *ACS Sustainable Chemistry & Engineering* **7** (8), 7844–7850.

Biesheuvel, P. & Van der Wal, A. 2010 Membrane capacitive deionization. *Journal of Membrane Science* **346** (2), 256–262.

Chang, J., Duan, F., Su, C., Li, Y. & Cao, H. 2020 Removal of chloride ions using a bismuth electrode in capacitive deionization (CDI). *Environmental Science: Water Research & Technology* **6** (2), 373–382.

Chen, R., Sheehan, T., Ng, J. L., Brucks, M. & Su, X. 2020 Capacitive deionization and electrosorption for heavy metal removal. *Environmental Science: Water Research & Technology* **6** (2), 258–282.

Choi, J., Dorji, P., Shon, H. K. & Hong, S. 2019 Applications of capacitive deionization: desalination, softening, selective removal, and energy efficiency. *Desalination* **449**, 118–130.

Fan, C.-S., Tseng, S.-C., Li, K.-C. & Hou, C.-H. 2016 Electro-removal of arsenic(III) and arsenic(V) from aqueous solutions by capacitive deionization. *Journal of Hazardous Materials* **312**, 208–215. doi.org/10.1016/j.jhazmat.2016.03.055.

Gabelich, C. J., Tran, T. D. & Suffet, I. M. 2002 Electrosorption of inorganic salts from aqueous solution using carbon aerogels. *Environmental Science & Technology* **36** (13), 3010–3019.

Gholami, M., Rasoulzadeh, H., Ahmadi, T. & Hosseini, M. 2020 Synthesis, characterization of nickel doped zinc oxide by radio-frequency sputtering and application in photo-electrocatalysis degradation of norfloxacin. *Materials Letters* **269**, 127647.

Guyes, E. N., Shocron, A. N., Simanovski, A., Biesheuvel, P. & Suss, M. E. 2017 A one-dimensional model for water desalination by flow-through selectrode capacitive deionization. *Desalination* **415**, 8–13.

Hassanvand, A., Chen, G. Q., Webley, P. A. & Kentish, S. E. 2018 A comparison of multicomponent electrosorption in capacitive deionization and membrane capacitive deionization. *Water Research* **131**, 100–109.

Hou, C.-H. & Huang, C.-Y. 2013 A comparative study of electrosorption selectivity of ions by activated carbon electrodes in capacitive deionization. *Desalination* **314**, 124–129.

Huyskens, C., Helsen, J. & de Haan, A. 2013 Capacitive deionization for water treatment: screening of key performance parameters and comparison of performance for different ions. *Desalination* **328**, 8–16.

Hwang, S.-W. & Hyun, S.-H. 2004 Capacitance control of carbon aerogel electrodes. *Journal of Non-Crystalline Solids* **347** (1–3), 238–245.

Ihsanullah, I., Atieh, M. A., Sajid, M. & Nazal, M. K. 2021 Desalination and environment: a critical analysis of impacts, mitigation strategies, and greener desalination technologies. *Science of the Total Environment* **780**, 146585.

Jiang, S., Wang, H., Xiong, G., Wang, X. & Tan, S. 2018 Removal of nitrate using activated carbon-based electrodes for capacitive deionization. *Water Supply* **18** (6), 2028–2034.

Jiang, J., Kim, D. I., Dorji, P., Phuntsho, S., Hong, S. & Shon, H. K. 2019 Phosphorus removal mechanisms from domestic wastewater by membrane capacitive deionization and system optimization for enhanced phosphate removal. *Process Safety and Environmental Protection* **126**, 44–52.

Job, N., Théry, A., Pirard, R., Marien, J., Kocon, L., Rouzaud, J.-N., Béguin, F. & Pirard, J.-P. 2005 Carbon aerogels, cryogels and xerogels: influence of the drying method on the textural properties of porous carbon materials. *Carbon* **43** (12), 2481–2494.

Johnson, A. & Newman, J. 1971 Desalting by means of porous carbon electrodes. *Journal of the Electrochemical Society* **118** (3), 510.

Kalfa, A., Shapira, B., Shopin, A., Cohen, I., Avraham, E. & Aurbach, D. 2020 Capacitive deionization for wastewater treatment: opportunities and challenges. *Chemosphere* **241**, 125003.

Khavarian-Garmsir, A. R., Pourahmad, A., Hataminejad, H. & Farhoodi, R. 2019 Climate change and environmental degradation and the drivers of migration in the context of shrinking cities: a case study of Khuzestan province, Iran. *Sustainable Cities and Society* **47**, 101480.

Kim, Y.-J., Kim, J.-H. & Choi, J.-H. 2013 Selective removal of nitrate ions by controlling the applied current in membrane capacitive deionization (MCDI). *Journal of Membrane Science* **429**, 52–57. doi.org/10.1016/j.memsci.2012.11.064.

Kim, N., Hong, S. P., Lee, J., Kim, C. & Yoon, J. 2019 High-desalination performance via redox couple reaction in the multichannel capacitive deionization system. *ACS Sustainable Chemistry & Engineering* **7** (19), 16182–16189.

Lee, M., Fan, C.-S., Chen, Y.-W., Chang, K.-C., Chiueh, P.-T. & Hou, C.-H. 2019 Membrane capacitive deionization for low-salinity desalination in the reclamation of domestic wastewater effluents. *Chemosphere* **235**, 413–422.

Liang, P., Yuan, L., Yang, Y., Zhou, S. & Huang, X. 2013 Coupling ion-exchangers with inexpensive activated carbon fiber electrodes to enhance the performance of capacitive deionization cells for domestic wastewater desalination. *Water Research* **47** (7), 2523–2530.

Martínez-Landeros, V., Hernandez-Como, N., Gutierrez-Heredia, G., Quevedo-López, M. A. & Aguirre-Tostado, F. 2019 Structural, chemical and electrical properties of CdS thin films fabricated by pulsed laser deposition using varying background gas pressure. *Thin Solid Films* **682**, 24–28.

Mossad, M. & Zou, L. 2013 Evaluation of the salt removal efficiency of capacitive deionisation: kinetics, isotherms and thermodynamics. *Chemical Engineering Journal* **223**, 704–713.

Pan, S.-Y., Haddad, A. Z., Kumar, A. & Wang, S.-W. 2020 Brackish water desalination using reverse osmosis and capacitive deionization at the water-energy nexus. *Water Research* **183**, 116064.

Panagopoulos, A. 2020 A comparative study on minimum and actual energy consumption for the treatment of desalination brine. *Energy* **212**, 118733.

Panagopoulos, A. 2021 Water-energy nexus: desalination technologies and renewable energy sources. *Environmental Science and Pollution Research* **28** (4), 1–14.

Panagopoulos, A. & Haralambous, K.-J. 2020 Environmental impacts of desalination and brine treatment-Challenges and mitigation measures. *Marine Pollution Bulletin* **161**, 111773.

Pastushok, O., Zhao, F., Ramasamy, D. L. & Sillanpää, M. 2019 Nitrate removal and recovery by capacitive deionization (CDI). *Chemical Engineering Journal* **375**, 121943.

Rasoulzadeh, H., Motesaddi Zarandi, S., Massoudinejad, M. & Amini, M. M. 2021a Modelling and optimisation by response surface technique for adsorption of carbon dioxide by aminated biosilica/alginate composite: experiments, characterisation and regeneration studies. *International Journal of Environmental Analytical Chemistry* **101**, 1–22.

Rasoulzadeh, H., Sheikhmohammadi, A., Abtahi, M., Alipour, M. & Roshan, B. 2021b Predicting the capability of diatomite magnano composite boosted with polymer extracted from brown seaweeds for the adsorption of cyanide from water solutions using the response surface methodology: modelling and optimisation. *International Journal of Environmental Analytical Chemistry* **101**, 1–14.

Rasoulzadeh, H., Sheikhmohammadi, A., Asgari, E. & Hashemzadeh, B. 2021c The adsorption behaviour of triclosan onto magnetic bio polymer beads impregnated with diatomite. *International Journal of Environmental Analytical Chemistry* **101**, 1–13.

Remillard, E. M., Shocron, A. N., Rahill, J., Suss, M. E. & Vecitis, C. D. 2018 A direct comparison of flow-by and flow-through capacitive deionization. *Desalination* **444**, 169–177.

Sarrafi, O., Faezi Ghasemi, M. & Chaichi Nosrati, A. 2016 Isolation and characterization of toxicogenic fungi strains from wheat and corn used in Kerman city. *Journal of Microbial World* **8** (4), 25.

Seo, S.-J., Jeon, H., Lee, J. K., Kim, G.-Y., Park, D., Nojima, H., Lee, J. & Moon, S.-H. 2010 Investigation on removal of hardness ions by capacitive deionization (CDI) for water softening applications. *Water Research* **44** (7), 2267–2275.

Son, M., Pothanamkandathil, V., Yang, W., Vrouwenvelder, J. S., Gorski, C. A. & Logan, B. E. 2020 Improving the thermodynamic energy efficiency of battery electrode deionization using flow-through electrodes. *Environmental Science & Technology* **54** (6), 3628–3635.

Sufiani, O., Tanaka, H., Teshima, K., Machunda, R. L. & Jande, Y. A. 2020 Enhanced electrosorption capacity of activated carbon electrodes for deionized water production through capacitive deionization. *Separation and Purification Technology* **247**, 116998.

Tang, W., Kovalsky, P., He, D. & Waite, T. D. 2015 Fluoride and nitrate removal from brackish groundwaters by batch-mode capacitive deionization. *Water Research* **84**, 342–349.

Tang, W., Kovalsky, P., Cao, B., He, D. & Waite, T. D. 2016 Fluoride removal from brackish groundwaters by constant current capacitive deionization (CDI). *Environmental Science & Technology* **50** (19), 10570–10579.

Tang, W., He, D., Zhang, C., Kovalsky, P. & Waite, T. D. 2017 Comparison of Faradaic reactions in capacitive deionization (CDI) and membrane capacitive deionization (MCDI) water treatment processes. *Water Research* **120**, 229–237.

Tang, W., Liang, J., He, D., Gong, J., Tang, L., Liu, Z., Wang, D. & Zeng, G. 2019 Various cell architectures of capacitive deionization: recent advances and future trends. *Water Research* **150**, 225–251.

Tang, K., Yiacoumi, S., Li, Y., Gabitto, J. & Tsouris, C. 2020 Optimal conditions for efficient flow-electrode capacitive deionization. *Separation and Purification Technology* **240**, 116626.

Uzun, H. I. & Debik, E. 2019 Economical approach to nitrate removal via membrane capacitive deionization. *Separation and Purification Technology* **209**, 776–781. https://doi.org/10.1016/j.seppur.2018.09.037.

Wang, L. & Lin, S. 2019 Mechanism of selective ion removal in membrane capacitive deionization for water softening. *Environmental Science & Technology* **53** (10), 5797–5804.

Wang, C., Song, H., Zhang, Q., Wang, B. & Li, A. 2015 Parameter optimization based on capacitive deionization for highly efficient desalination of domestic wastewater biotreated effluent and the fouled electrode regeneration. *Desalination* **365**, 407–415.

Wang, L., Dykstra, J. & Lin, S. 2019 Energy efficiency of capacitive deionization. *Environmental Science & Technology* **53** (7), 3366–3378.

Xing, W., Liang, J., Tang, W., Zeng, G., Wang, X., Li, X., Jiang, L., Luo, Y., Li, X. & Tang, N. 2019 Perchlorate removal from brackish water by capacitive deionization: experimental and theoretical investigations. *Chemical Engineering Journal* **361**, 209–218. doi.org/10.1016/j.cej.2018.12.074.

Xing, W., Liang, J., Tang, W., He, D., Yan, M., Wang, X., Luo, Y., Tang, N. & Huang, M. 2020 Versatile applications of capacitive deionization (CDI)-based technologies. *Desalination* **482**, 114390.

Xu, P., Drewes, J. E., Heil, D. & Wang, G. 2008 Treatment of brackish produced water using carbon aerogel-based capacitive deionization technology. *Water Research* **42** (10–11), 2605–2617.

Yeo, J.-H. & Choi, J.-H. 2013 Enhancement of nitrate removal from a solution of mixed nitrate, chloride and sulfate ions using a nitrate-selective carbon electrode. *Desalination* **320**, 10–16.

Zhang, C., He, D., Ma, J., Tang, W. & Waite, T. D. 2019a Comparison of faradaic reactions in flow-through and flow-by capacitive deionization (CDI) systems. *Electrochimica Acta* **299**, 727–735.

Zhang, C., Wang, X., Wang, H., Wu, X. & Shen, J. 2019b A positive-negative alternate adsorption effect for capacitive deionization in nano-porous carbon aerogel electrodes to enhance desalination capacity. *Desalination* **458**, 45–53.

Zhao, Y., Wang, Y., Wang, R., Wu, Y., Xu, S. & Wang, J. 2013 Performance comparison and energy consumption analysis of capacitive deionization and membrane capacitive deionization processes. *Desalination* **324**, 127–133.

Zhao, X., Wei, H., Zhao, H., Wang, Y. & Tang, N. 2020 Electrode materials for capacitive deionization: a review. *Journal of Electroanalytical Chemistry* **873**, 114416.